infrastructures

MDPI

Article

An Analytical Method for Determining the Stress–Strain State of a Subgrade with Combined Reinforcement

Ahmad Alkhdour [1], Oleksii Tiutkin [2], Szabolcs Fischer [3,*] and Dmytro Kurhan [2]

[1] Department of Civil Engineering, Al-Balqa Applied University, Al-Salt 19117, Jordan; a.alkhdour@bau.edu.jo
[2] Department of Transport Infrastructure, Ukrainian State University of Science and Technologies, UA-49010 Dnipro, Ukraine; o.l.tiutkin@ust.edu.ua (O.T.); d.m.kurhan@ust.edu.ua (D.K.)
[3] Central Campus Győr, Széchenyi István University, H-9026 Győr, Hungary
* Correspondence: fischersz@sze.hu

Abstract: This article presents the fundamentals of an analytical method for determining the stress–strain state of a railway subgrade reinforced with geosynthetic material. The reinforcement described is a combined system where the geosynthetic material forms an open shell containing a layer of compacted crushed stone. The overall stress–strain state is proposed to be viewed as a superposition of two states of the subgrade. The stresses and displacements in the first state refer to the unreinforced subgrade (matrix), while the stress–strain state of the reinforcement element is determined using analytical constructs from composite theory. The dependencies of the overall stress–strain state are applied in a numerical analysis, which confirms the positive effect of reduced subgrade deformations. A small-scale experimental model further validates the accuracy of the analytical approach.

Keywords: railway; subgrade; geosynthetic materials; combined reinforcement; stress–strain state; analytical method; numerical analysis

Citation: Alkhdour, A.; Tiutkin, O.; Fischer, S.; Kurhan, D. An Analytical Method for Determining the Stress–Strain State of a Subgrade with Combined Reinforcement. *Infrastructures* **2024**, *9*, 240. https://doi.org/10.3390/infrastructures9120240

Academic Editor: Giuseppe Cantisani

Received: 31 October 2024
Revised: 9 December 2024
Accepted: 18 December 2024
Published: 23 December 2024

1. Introduction

Soil, a building material for constructing a subgrade, is not a structural material. This means that the construction properties of soil depend on its origin, the features of its formation, and the characteristics of the technology by which the soil acquires the predicted parameters. There is no doubt that the construction of long structures, such as the subgrade of railways or highways, cannot ensure the same soil parameters (density, modulus of elasticity, porosity coefficient, optimal humidity, etc.) along the entire length [1–3]. Compaction technology during the construction of the subgrade may yield errors when erecting this structure in height.

Thus, two general factors, namely the properties of the soil before construction and the accumulation of technological errors during construction, form the situation before the start of operation of the railway subgrade. Even with the implementation of proven technology, the presence of non-homogeneous or overly porous soil could lead to an unsatisfactory result [4,5]. Conversely, soil with sufficiently high qualities but using a compaction technology that provides a significant dispersion of properties after its application can achieve only a mediocre quality of the subgrade [6]. In the paper [7], the results of experimental studies on sleeper performance within weak subgrades are presented. The analysis of ballast loads reveals specific interactions between the railway and rolling stock in such areas. The paper [8] demonstrates the relationship between the reduction in the lateral stability of the railway track and the weakening of the ballast and soil. The paper [9] presents a mathematical model of track and rolling stock interaction on sections with weak soil. The study [10] examines the degradation of railway track conditions due to insufficient ballast and soil strength caused by natural factors.

The totality of these factors, as well as their somewhat unpredictable combination, leads to the fact that before the start of operation of the subgrade, it may already have

defects. These defects during operation lead to deformations of the ballast prism, the penetration of crushed stone into the loam of the subgrade, an increased deformation of slopes, and local landslides associated with overwetting, and they accordingly require timely repair. Since it is no longer possible to compact the subgrade soil, the repair involves correcting the path, increasing the thickness of the ballast, and compacting it. Accordingly, the cycle of penetration of ballast into the subgrade soil begins again [11–13].

The deformed state of the subgrade constructed from sandy or clay soils will differ from that of loamy soils. The primary parameter affecting deformation is the elastic modulus, which varies among these soil types. However, loamy soil was chosen because it is prescribed by construction regulations as the main material for constructing railway subgrades. These regulations prohibit the use of clay soil and limit the use of sandy soil, which is employed only as a leveling material.

Such a pattern of operation is objectively predetermined, since the modulus of elasticity of crushed stone ballast is approximately 3.0–3.2 times greater than the modulus of elasticity of the compacted loam of the subgrade. If the rail-sleeper grid works as a system of beams on an elastic base, then the stress in the ballast, which has lost its shape during operation and increases in local areas, and the ballast particles destroy the subgrade. After a certain level of overstressing of the subgrade, it begins to deform intensively and needs new repair.

Strengthening can improve the operation of subgrades that have defects and deformations. Over almost a century of operation of European railways, considerable experience in applying various reinforcement techniques has been accumulated. It should be noted that this research field is developing quite actively, receiving innovative developments that change the understanding of the general concept of improving the operation of the subgrade and the railway track as a whole [14–17].

The main technique of strengthening the railway subgrade, which prevails even today, is using geosynthetic materials (geotextile, geogrid, geomats for various purposes, etc.) [18–21]. The arrangement of geosynthetic materials in the body of the subgrade or on the border of the ballast prism has a serious theoretical justification and considerable practical experience. The results of this experience indicate that the use of geosynthetic materials has a positive effect on reducing the deformed state of the subgrade and improving its overall operation.

However, in recent decades, the use of geosynthetic materials has increasingly shifted to the area of separation rather than reinforcement. Thus, geonets and geogrids are applied to separate crushed stone ballast and subgrade soil. The reinforcing role of geosynthetic materials, in this case, is reduced. However, using these materials to separate the ballast and the subgrade is also characterized by positive results. Using geonets and geogrids significantly reduces the penetration of crushed stone particles into the subgrade soil, eventually reducing the deformation situation.

Together with geosynthetic materials located in the body of the subgrade or on the border with ballast horizontally, vertical reinforcement elements have played an increasingly important role in the last two decades. Such elements are piles or micropiles created on the base of drilling injection or drilling mixing technologies [22,23]. These technologies and the elements created on their basis are transferred from the strengthening of soil foundations in civil construction and have also been significantly theoretically developed and widely applied in practice. In the last decade, scientific papers have even appeared that outline the issues of revising the use of geosynthetic materials based on the positive experience of reducing the vertical component of deformation using piles or micropiles.

The third direction of strengthening the subgrade of railways is the use of layers that deform little, namely compacted crushed stone, crushed stone, asphalt of hot or cold laying, etc. [24–26]. Based on a reinforcement idea different from submerging geosynthetic materials and placing vertical reinforcement elements, this direction already has sufficient scientific justification to be considered as a potential way to improve railway operation. In addition, the combination of geogrids and geonets at the border of the ballast and subgrade, together with piles created based on drilling injection or drilling mixing technologies, is

starting to be used quite widely. Such a combination works in two directions of reinforcement, i.e., the vertical elements reduce the vertical component of deformation, while the separation of the ballast and subgrade minimizes the penetration of ballast particles [27,28].

Although geosynthetic materials are no longer dominant in strengthening the railway subgrade, their potential cannot be considered exhausted. The development of this potential is seen in the design of new reinforcement structures based on geosynthetic materials and their combination with other reinforcement techniques to increase efficiency. It is believed that this increase can be achieved by anchoring the geosynthetic fabric, effectively creating a protective shell. Modification of the proposed combined subgrade reinforcement system is possible by replacing the geosynthetic material of the unsealed shell from the fabric to the geogrid. Such a modification, due to the higher strength and stiffness of the geogrid, will enhance the overall strength and stiffness of the combined reinforcement. This improvement in key operational parameters will help account for the effects of extreme weather conditions or seasonal changes. Moreover, combining geosynthetic material and a low-deformable layer, a compacted layer of crushed stone–soil mixture is arranged inside such a shell.

The structure of this paper reflects its complex nature. The second section consists of an analytical study of the stress–strain state of railway subgrade reinforcement utilizing an open shell made of geosynthetic materials filled with a crushed stone–soil mixture. The third section is divided into two parts. The first part presents the implementation of the developed analytical concepts for applying models based on the finite element method, accompanied by examples of numerical results. The second part of the third section contains the results of experimental investigations of the combined reinforcement, demonstrating the adequacy of the analytical studies. Thus, this paper aims to conduct a comprehensive theoretical and practical investigation of the stress–strain state of railway subgrade reinforcement using an open shell made of geosynthetic materials filled with a crushed stone–soil mixture.

2. Materials and Methods

2.1. Prerequisites for the Analytical Determination of the Stress–Strain State

The essence of the combined strengthening technique is the connection of two elements in one scheme that are fundamentally different in properties and strengthening action, but in a single complex, their influence is the most significant. It should be noted that by combining geotextiles with bends (unclosed shell) and a layer of slightly deformed material (stone–soil mixture) located between two fabrics in a single strengthening scheme, it became possible to achieve the maximum strengthening effect. When two reinforcing elements are combined, there is such an interaction between them that if they acted individually, the sum of their interactions would not coincide with the overall interaction of the combined system (see Figure 1).

Accordingly, when the load on the main platform of the model is increased, the resulting stresses affect the bends of the shell, and the upper layer of soil with an additional load leads to the restraining effect. Sufficiently long bends make it possible to develop significant frictional forces on the outer surface (subgrade soil—geotextile) and the inner surface (geotextile—crushed stone–soil mixture). The restraining effect increases in proportion to the increase in the load on the main platform of the model and, accordingly, the friction on the specified surfaces increases, as represented in Figure 1.

It was found out earlier that the closure of the geotextile fabric practically does not change the stress–strain state of the model, which is explained by the fact that the friction on a certain length of the end of the shell is sufficient to prevent the geotextile from shifting or pulling out. The share of friction that falls on the middle of the shell does not significantly impact this effect, so the open shell with bends is correctly perceived as a fictitious closed shell.

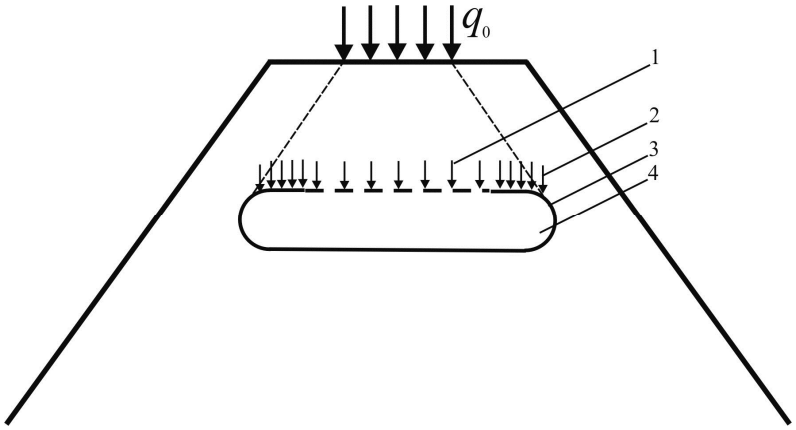

Figure 1. Schematic showing the shell made of geosynthetic material considering the restraining effect: 1—loading, transmitted on the strengthening element (part of the train load and natural weight); 2—load transmitted to the shell bend; 3—fictitiously closed geotextile shell; 4—filler (stone–soil mixture).

Accordingly, an important direction in developing analytical methods for determining the stress–strain state of the subgrade with combined reinforcement is considering the interaction between the reinforcement elements and the search for features. Based on the premise of the interaction between the reinforcing element and the subgrade soil, several possible options for developing analytical provisions should be reviewed, which would make it possible to solve the problem of finding stresses and deformations both in the system as a whole and its elements.

The subgrade with combined reinforcement can be viewed as consisting of the soil matrix and the reinforcing element. The latter cannot be called an armature and is considered as such since it is not such an element, being a geotextile bag with a layer of crushed stone–soil mixture placed inside the shell. It should also be noted that the matrix is represented as uniform in height. The reinforcing element in a simplified form can also be represented as uniform. This element is distinguished by increased deformation properties, and when it interacts with the matrix, it causes a disturbance of the stress–strain state in its vicinity, caused by a jump in these properties.

Having divided the system into a matrix and a reinforcing element, it is possible to explain the interaction between them using the principle of superposition. The total stressed state of the matrix and reinforcing element system consists of the sum of two stressed states—intact and removed. In this case, the intact stressed state will be the state in the subgrade caused by its natural weight and the train load, and the removed stressed state will be the one that reduces or redistributes the stress of the embedded reinforcing element. However, it should be considered that superposition is possible only for the general system "matrix–reinforcing element", and the search for the stress–strain state of the reinforcing element should be carried out from the viewpoint that it is a composite element. That is, in the strengthening element itself, which in the studied form is a self-supporting structure, there is a complex interaction between the geotextile and the filler (stone–soil mixture), which in a more simplified form is transferred to the interaction with the matrix.

Accordingly, having determined the stress–strain state of the intact subgrade, it can be corrected by subtracting certain stress tensors and deformations determined during the analytically calculated stress–strain state of the reinforcing element.

Before proceeding to specific analytical constructions, it is necessary to define the hypotheses that will be involved in the solution, since the complexity of the interaction is unambiguous.

1. The problem statement is flat; the condition of flat deformation is fulfilled. This statement is not a simplification that significantly affects the understanding of the physical meaning of the accumulation of stresses and the development of deformations in the

reinforced subgrade under the influence of the train load, since the distribution of stresses and deformations along the axis of the train movement is minimal compared to the factors of the same name acting in the transverse plane (the share of these factors in the total stress–strain state is no more than 5–7%). Deformations, as stated, are equal to zero; thus, the analytical solution is significantly simplified.

2. The subgrade soil is assumed to be homogeneous and isotropic. As already stated above, the use of such a hypothesis is legitimate. A layer of crushed stone–soil mixture is also considered as a homogeneous isotropic material, filling the open geotextile shell. Furthermore, this reinforcing low-deformation layer of crushed stone–soil mixture is assumed to be compacted to such a degree that its deformations can be neglected, with its geometric dimensions (thickness and length) remaining unchanged under train loading.
3. The geotextile material, which encloses a low-deformation layer of crushed stone–soil mixture, is assumed to be elastic and isotropic, does not perceive compressive stresses, and has a certain tensile strength. The bending stiffness of the reinforcing geotextile element is assumed to be zero, and the stress state is defined as membrane stress.

Bringing the analytical problem to the elastic formulation is expedient and is explained by the fact that during real operation of the subgrade, the emergence of plastic deformations is unacceptable and requires repair or reconstruction measures. However, for a more comprehensive account of the formation of a stress–strain state, especially in some characteristic places of the considered subgrade, it is necessary to expand the purely elastic formulation using a slightly different approach. Given that solving the elastoplastic problem would significantly complicate analytical constructions, yet it is crucial to account for plastic deformations, the mixed problem of elasticity and plasticity theory will be applied as a method.

The essence of the mixed problem of the theory of elasticity and plasticity is the provision of the simultaneous existence in the structure, in this case in the subgrade, of areas of elastic sublimit and plastic beyond-limit deformations. Accordingly, for each area, it is possible to apply its own theory; for the sublimit area—elasticity (this also applies to the analytical solution, in general, when the level is stressed to the limit of elasticity)—and for the beyond-limit area—plasticity. The simultaneous application of both theories is expedient only after the emergence of regions of plastic deformation; until that time, the elastic formulation of the problem is entirely correct.

An essential point in solving the mixed problem of the theory of elasticity and plasticity is finding the zones of different types of deformation using the conditions of the transition of the subgrade soil from the elastic stage to the plastic stage, for example, using the Coulomb–Mohr envelope equation.

The most crucial advantage in applying the mixed problem of the theory of elasticity and plasticity is that in addition to the proven adequacy of the analytical solutions obtained by experimental and natural data, its analytical constructions are pretty simple to implement with the help of numerical methods. Thus, the application of such a problem is sufficiently entirely and in detail developed for the finite element method.

2.2. Approach to Determining the Intact Stress–Strain State in an Unreinforced Subgrade

The inherent stresses of the subgrade and the stresses from the train load primarily impact its operational reliability. Existing analytical methods for calculating the stress in the subgrade are most often based on the laws of the theory of elasticity. As it has already been clarified, this approach to determining the intact stress–strain state in an unreinforced subgrade is legitimate, since when determining the stress from the soil's natural weight and the train load, it can be assumed that the upper part of the subgrade is in a state of prelimit equilibrium, as well as the main requirement for the subgrade being a requirement for the absence of final deformations.

To determine the components of the stressed state, an elementary layer of thickness $d\xi$ was selected in the subgrade and considered as a uniformly distributed load, with the train load also applied, as shown in Figure 2.

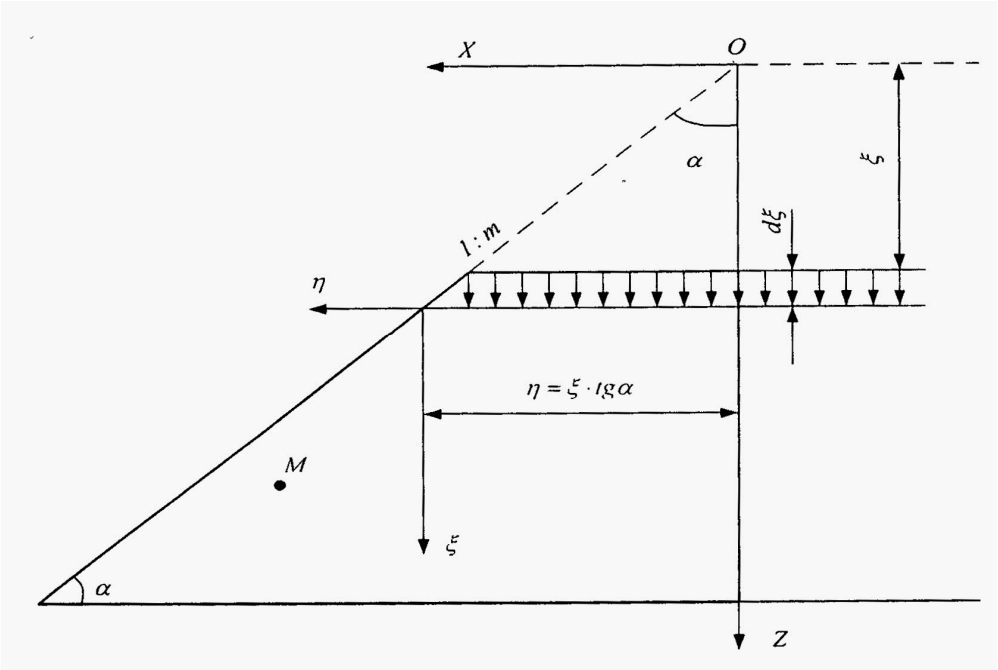

Figure 2. Calculation scheme for determining the intact stressed state in the subgrade.

The stressed state at an arbitrary point of the massif with coordinates z and x satisfies the classical equations of equilibrium.

$$\frac{\partial \sigma_z}{\partial z} + \frac{\partial \tau_{xz}}{\partial x} = -\gamma \sigma_z(z, x); \tag{1}$$

$$\frac{\partial \sigma_x}{\partial x} + \frac{\partial \tau_{xz}}{\partial z} = -\gamma \sigma_x(z, x), \tag{2}$$

where σ_x, σ_z, and τ_{xz} are the normal stresses along axes x and z and tangential in the plane xz, respectively; $\gamma\sigma_z(z, x)$ and $\gamma\sigma_x(z, x)$ are projections of volumetric forces on the corresponding axes; and γ is the specific weight of the subgrade soil without reinforcement.

In addition to the equilibrium equations, the deformation condition was introduced.

$$\nabla^2 \sigma(z, x) = -\gamma \left[\frac{\partial \sigma(z, x)}{\partial x} + \frac{\partial \sigma(z, x)}{\partial z} + \frac{\partial \sigma(z, x, \xi)}{\partial z} \right], \tag{3}$$

where ∇ is the Laplace operator.

The solution to the reduced equations in partial derivatives is similar to M. Levy's solution to this type of equation.

$$\sigma_{z(z-\xi, x-\eta)} = -\frac{q}{tg\alpha + \pi - \alpha} \left[tg\alpha + \left(\frac{\pi}{2} - \alpha \right) - arctg \frac{x - \eta}{z - \xi} - \frac{(z - \xi)(x - \eta)}{(z - \xi)^2 + (x - \eta)^2} \right]; \tag{4}$$

$$\sigma_{x(z-\xi, x-\eta)} = -\frac{q}{tg\alpha + \pi - \alpha} \left[\left(\frac{\pi}{2} - \alpha \right) - arctg \frac{x - \eta}{z - \xi} + \frac{(z - \xi)(x - \eta)}{(z - \xi)^2 + (x - \eta)^2} \right]; \tag{5}$$

$$\tau_{xz(z-\xi, x-\eta)} = -\frac{q}{tg\alpha + \pi - \alpha} \cdot \frac{(z - \xi)^2}{(z - \xi)^2 + (x - \eta)^2}, \tag{6}$$

where q is the load on the main subgrade site from the fictitious wedge and α, ξ and η are geometric parameters of the subgrade, as shown in Figure 2.

By integrating ξ over the range from 0 to z, the following expressions were obtained:

$$\sigma_z = \frac{q}{tg\alpha+\pi-\alpha}\left[\left[-\left(\frac{\pi}{2}-\alpha\right)\left(1-2cos^2\alpha\right)sin^2\alpha + sin^2\alpha\cdot tg\alpha + \frac{\pi}{2}cos^2\alpha\right]z + sin\alpha cos\alpha\left[2\left(\frac{\pi}{2}-\alpha\right)sin^2\alpha + \frac{\pi}{2}\right]\right.$$
$$x + 2sin^4\alpha(z\cdot ctg\alpha - x)ln\frac{z\cdot ctg\alpha}{r} + sin\alpha(z\cdot sin\alpha + x\cdot cos\alpha)arctg\frac{x}{z} - 2cos\alpha\, sin^3\alpha(z\cdot ctg\alpha - x) \quad (7)$$
$$\left. arctg\frac{z\cdot sin\alpha + x\cdot cos\alpha}{sin\alpha(z\cdot ctg\alpha - x)}\right];$$

$$\sigma_x = \frac{q}{tg\alpha+\pi-\alpha}\left[\left[-\left(\frac{\pi}{2}-\alpha\right)\left(1-2cos^2\alpha\right)sin^2\alpha + sin\alpha\cdot cos\alpha + \frac{\pi}{2}cos^2\alpha\right]z - sin\alpha cos\alpha\left[2\left(\frac{\pi}{2}-\alpha\right)sin^2\alpha - \frac{\pi}{2}\right]\right.$$
$$x + 2cos^2\alpha\cdot sin^2\alpha(z\cdot ctg\alpha - x)ln\frac{z\cdot ctg\alpha}{r} + sin\alpha(z\cdot sin\alpha + x\cdot cos\alpha)arctg\frac{x}{z} + 2cos\,\alpha\, sin^3\alpha(z\cdot ctg\alpha - x) \quad (8)$$
$$\left. arctg\frac{z\cdot sin\alpha + x\cdot cos\alpha}{sin\alpha(z\cdot ctg\alpha - x)}\cdot ln\frac{z\cdot ctg\alpha - x}{r}\right];$$

$$\tau_{xz} = \frac{q}{tg\alpha+\pi-\alpha}\left[-z\, sin^2\alpha + 2\, cos\,\alpha\, sin^3\alpha(z\cdot ctg\alpha - x)\cdot ln\frac{z\cdot ctg\alpha - x}{r} - cos^2\alpha\cdot\right.$$
$$\left. sin^2\alpha(z\cdot ctg\alpha - x)\cdot\left[\left(\frac{\pi}{2}-\alpha\right) + arctg\frac{z\cdot sin\alpha + x\cdot cos\alpha}{sin\alpha(z\cdot ctg\alpha - x)}\right]\right], \quad (9)$$

where $r = \sqrt{z^2 - x^2}$.

In accordance with the condition of joint deformations, the following is obtained:

$$\sigma_{x(x,z,r)} = const = q\frac{tg\alpha + \left(\frac{\pi}{2}-\alpha\right)}{tg\alpha + (\pi-\alpha)}; \quad (10)$$

$$\frac{\partial}{\partial z}\sigma_{x(x,z,\xi)|\xi=r} = 0 \quad (11)$$

and the compatibility identity, Expression (3), takes the form

$$\nabla^2\sigma(z,x) = -\gamma\frac{\partial}{\partial z}\sigma_{x(x,z,\xi)} = \frac{2\gamma}{tg\alpha + \pi - \alpha}\cdot\frac{1}{z\cdot ctg\alpha - x}. \quad (12)$$

The vertical stresses at any point of the subgrade are found from the following expression:

$$\sigma_z = \sigma_{tl} + \sigma_\gamma, \quad (13)$$

where σ_{tl} is the tension component caused by the action of the temporary load and σ_γ is the stress component caused by the action of the soil's natural weight.

$$\sigma_\gamma = -\gamma\frac{z}{2}\left(1 - \frac{h_0^2}{z^2}\right). \quad (14)$$

From the theory of elasticity, it is known that for a uniformly distributed load on the main area of the subgrade, the vertical stresses are equal to

$$\sigma_{tl} = -\frac{q_0}{\pi}\left(\beta_1 + \frac{1}{2}sin^2\beta_1 - \beta_2 + \frac{1}{2}sin^2\beta_2\right), \quad (15)$$

where q_0 is the intensity of the train load and β_1 and β_2 are the angles defining the position of the point in the subgrade and laid off from the verticals extended from the beginning and end of the distributed load.

However, such a solution becomes somewhat unsatisfactory for points that lie closer to the slope boundaries, as concentrations of stress arising in them are slightly overestimated. Therefore, to clarify the stresses in the near-slope zone (in the absence of plastic regions), one can use the Christensen method, a special case of a mixed problem of the elasticity and plasticity theory, as represented in Figure 3.

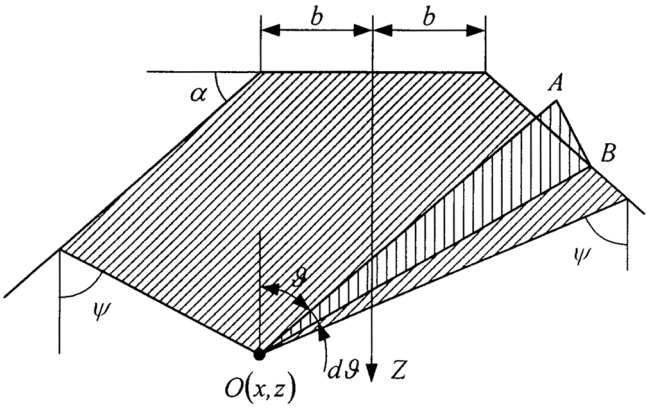

Figure 3. The calculation scheme for the Christensen method.

Then, for the points of a given zone, the stresses are calculated using approximate equations.

$$\sigma_z = \gamma H\left[4\sigma_z'(1-\lambda) + \sigma_z''(4\pi - 3)\right]; \quad (16)$$

$$\sigma_x = \gamma H\left[4\sigma_x'(1-\lambda) + \sigma_x''(4\pi - 3)\right]; \quad (17)$$

$$\tau_{xz} = \gamma H\left[4\tau_{xz}'(1-\lambda) + \tau_{xz}''(4\pi - 3)\right], \quad (18)$$

where H is the subgrade height; λ is the lateral thrust coefficient determined through Poisson's ratio; $\lambda = \frac{\mu}{1-\mu}$; σ_z', σ_x', and τ_z' are the dimensionless stresses at any point of the considered region at $\lambda = 0.75$; and σ_z'', σ_x'', and τ_z'' are the dimensionless stresses at any point of the considered region at $\lambda = 0.1$.

Two methods can be used to control the formation of plastic regions in the analytical solution to the mixed problem of determining the intact stressed state in an unreinforced subgrade. The first is analytical and involves determining the region of plastic deformation using an elastic assessment based on the von Mises criterion, i.e., determining the geometric location of points with constant energy of distortion. However, this method is convenient for numerical solutions when it is sufficient to simply determine the total deformation energy using an application complex and visually separate the plastic zone as a place with constant energy of distortion.

The second method is simpler, since it is semi-analytical and is associated with the definition and verification of the stressed state of the near-slope zones with the condition of limit equilibrium in the form of a rectilinear envelope of the largest stress circles (Mohr circles), which is constructed based on the results of tests of real soils of the subgrade.

$$\sqrt{(\sigma_z - \sigma_x)^2 + 4\tau_{xz}^2} - (\sigma_z + \sigma_x)sin\phi = 2C \cdot cos\phi, \quad (19)$$

where ϕ and C are the angle of internal friction and the specific cohesion of the subgrade soil, respectively.

If, when substituting stresses from Formulas (16)–(18), the value of the right-hand part does not exceed the value of the left-hand part, then the subgrade soil is in a plastic state.

Having solved the problem of determining the stressed state, using the generalized Hooke's law reduced to the condition of flat deformation, the deformed state is found (the inverse problem of determining the stress–strain state), which does not present any particular difficulties with known values of the deformation modulus (the values are determined during compression or stabilometrical tests) and Poisson's ratio.

2.3. Stress–Strain State of the Reinforcing Element

The stress–strain state of the reinforcing element is determined based on its operation as a composite, since an open geotextile shell with filler in the form of a crushed stone–soil mixture can be considered as a three-layer package with seriously different properties of the shell and filler. It should be noted that an open shell can be considered fictitiously closed, following the nature of its deformation determined during the experiments.

The deformation pattern of the reinforcing element under the impact of a train load changes as follows: the filler in the form of a crushed stone–soil mixture, which has a high density and is practically incompressible, being separated from the matrix of the subgrade by a shell, cannot change volume (see Figure 1). Accordingly, the reinforcing element is deformed only together with the matrix, and its base is the subgrade with elastic properties. The positive effect of strengthening in such a combined way is that practically all the energy of deformation up to a certain limit is spent on an attempt to deform the reinforcing element, which dissipates or distributes it due to its design into friction forces and uniform distribution of deformations along its base (see Figure 4).

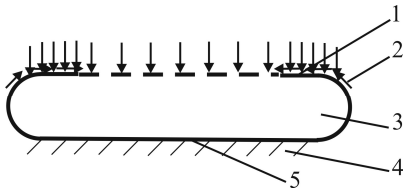

Figure 4. Stress and friction force distribution diagram in the reinforcing element: 1—clamped bend of the geotextile shell; 2—friction forces; 3—the compression zone of filler; 4—the elastic base; 5—the stretched fiber of the geotextile shell.

This scheme (see Figure 4) should be transformed into a design one, based on the above provisions on the formation of the stress–strain state (see Figure 5). This reinforcing element is represented as a fictitious closed shell with a filler consisting of several zones. At the top of the shell, it is the zone of the fictitious upper fiber with a length l_f and the zone of two bends with a length n, which are considered immobile; at the bottom, this is the zone of the lower fiber with a length r and a transition zone with a length $(l - r)$. The shell of the reinforcing element operates, as already described above, as a single whole.

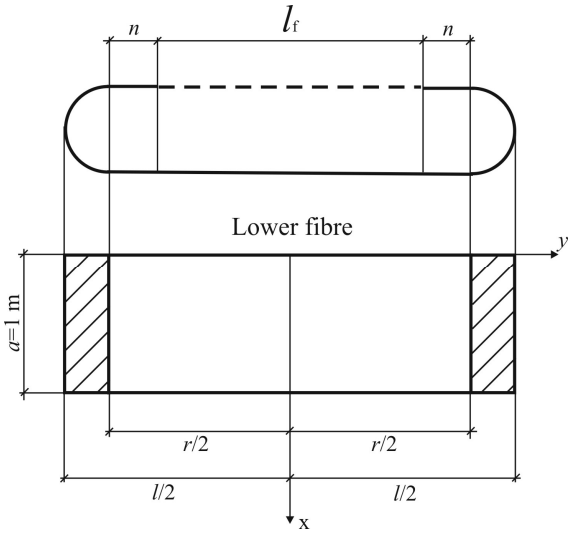

Figure 5. Calculation scheme for determining displacements and stresses in a reinforcing element (shell with filler).

The deflection of such a three-layer composite package of symmetrical structure, resting on an elastic foundation with known parameters, is approximately determined from the following equations:

- For the central line of the reinforcing element, coinciding with the axis x:

$$w = \frac{4q_0a^4}{D_T\pi^5}\sum_{m=1,3,5}^{\infty}\frac{E_m}{m^5P_m}(1 + A_m - B_m)sin\frac{m\pi x}{a}; \quad (20)$$

- For the lower fiber without transition zone $y \in \left(-\frac{r}{2}; \frac{r}{2}\right)$:

$$w = \frac{4q_0a^4}{D_T\pi^5}\sum_{m=1,3,5}^{\infty}\frac{1}{m^5P_m}\left[\left(1 + A_m ch\frac{m\pi y}{a_m} - B_m ch\frac{m\pi y}{a}\right) - E_m\left(\frac{C_{m1}}{ch\beta_{m1}}ch\frac{m\pi y}{a} - \frac{C_{m2}}{ch\beta_m}ch\frac{m\pi y}{a}\right)\right]sin\frac{m\pi x}{a}; \quad (21)$$

- For the transition zone of the lower $y \in \left[-\frac{l}{2}; -\frac{r}{2}\right] \cup \left[\frac{r}{2}; \frac{l}{2}\right]$:

$$w = \frac{4q_0a^4}{D_T\pi^5}\sum_{m=1,3,5}^{\infty}\frac{1}{m^5P_m}\left[\left(1 + A_m ch\frac{m\pi y}{a} - B_m ch\frac{m\pi y}{a}\right) - F_{m1}\left(G_m sh\frac{m\pi y}{a} - G_{m1}ch\frac{m\pi y}{a} - H_m sh\frac{m\pi y}{a} + H_{m1}ch\frac{m\pi y}{a}\right)\right]sin\frac{m\pi x}{a}0, \quad (22)$$

where a is the width along the axis x, taken equal to 1 m; D_T is the bending stiffness of the reinforcing element; P_m, a_m, β_{m1}, and β_m are the parameters of the three-layer reinforcing element; and A_m, B_m, E_m, C_{m1}, C_{m2}, G_m, G_{m1}, F_{m1}, H_m, and H_{m1} are constant coefficients.

Since the thickness of the geotextile shell does not affect the bending, the bending stiffness of the reinforcing element is determined as

$$D_T = \frac{c_{ssm}E_{ssm}}{12\left(1 - \nu_{ssm}^2\right)}, \quad (23)$$

where E_{ssm}, ν_{ssm}, and c_{ssm} are, respectively, the deformation modulus, Poisson's ratio, and the thickness of the crushed stone–soil mixture layer in the shell.

The parameters of the three-layer reinforcing element are determined from the following formulas:

$$P_m = 1 + 2\frac{B^2a^2}{D_Tm\pi^2}; a_m = a|P_m|^{-\frac{1}{2}}; B = \sqrt{\frac{c_{ssm}G_{ssm}}{2}}; \beta_m = 0,5\frac{m\pi r}{a}; \beta_{m1} = 0,5\frac{m\pi r}{a_m},$$

where G_{ssm} is the shear modulus of the crushed stone–soil mixture in the shell.

The constant coefficients in Formulas (20) and (21) take the following form:

$$A_m = \frac{a_m^2}{a^2 - a_m^2} \cdot \frac{1}{ch\alpha_{m1}}; B_m = \frac{a^2}{a^2 - a_m^2} \cdot \frac{1}{ch\alpha_m};$$
$$C_{m1} = \frac{a}{a^2 - a_m^2} \cdot (sh\beta_m - th\alpha_{m1}ch\beta_{m1})ch\beta_{m1};$$
$$C_{m2} = \frac{a}{a^2 - a_m^2} \cdot (sh\beta_m - th\alpha_m ch\beta_m)ch\beta_m;$$
$$\alpha_m = 0,5m\pi l; \alpha_{m1} = 0,5\frac{m\pi l}{a_m};$$
$$E_m = \frac{1}{1 + \frac{C_m k\pi m}{2D_TP_m}};$$
$$F_{m1} = (1 + A_{m1} - B_{m1})\left[(C_{m1} - C_m) + \frac{D_TP_m}{km\pi}\right]^{-1};$$
$$C_m = \frac{a \cdot th\alpha_m - a_m \cdot th\alpha_{m1}}{a^2 - a_m^2};$$
$$G_m = \frac{a_m}{a^2 - a_m^2}ch\beta_{m1};$$
$$G_{m1} = G_m th\alpha_{m1};$$
$$H_m = \frac{a}{a^2 - a_m^2}ch\beta_m; H_{m1} = H_m th\alpha_m,$$

where l is the length of the reinforcing element with transition areas and k is the coefficient of elastic resistance of the subgrade soil.

The stresses in the reinforcing element are equal for the lower fiber without a transition zone $y \in \left(-\frac{r}{2}; \frac{r}{2}\right)$.

$$\sigma_x = \pm\frac{4q_0a^2}{\pi^3 t_g}\sum_{m=1,3,5}^{\infty}\frac{1}{m^3P_m}\left[1 + L_m\left(1 - \nu_g\frac{a^2}{a_m^2}\right)ch\frac{m\pi y}{a_m} - N_m(1-\nu_g)ch\frac{m\pi y}{a}\right]sin\frac{m\pi x}{a}; \quad (24)$$

$$\sigma_y = \pm\frac{4q_0a^2}{\pi^3 t_g}\sum_{m=1,3,5}^{\infty}\frac{1}{m^3P_m}\left[\nu + L_{m1}\left(\nu_g - \frac{a^2}{a_m^2}\right)ch\frac{m\pi y}{a_m} - N_{m1}(\nu_g - 1)ch\frac{m\pi y}{a}\right]sin\frac{m\pi x}{a}, \quad (25)$$

where t_g and ν_g are the thickness and Poisson's ratio of the geotextile and L_m, N_m, L_{m1}, and N_{m1} are constant coefficients that are defined as

$$L_m = A_m + F_{m1}G_{m1}; N_m = C_m + F_{m1}G_{m1};$$
$$L_{m1} = B_m + F_{m1}G_{m1}; N_{m1} = E_m + F_{m1}G_{m1}.$$

For the transition zone, stresses should be found from a problem that considers delamination, the solution given below, with special attention given to the critical load of delamination. To carry out practical calculations, it is sufficient to enter the data on the analytical provisions into the main resolving equations of the numerical method (for example, the finite element method) and take 2–3 terms of the series.

2.4. Implementation of the Developed Analytical Provisions in the Finite Element Method

The most appropriate practical solution for the implementation of analytical provisions in the finite element method (FEM) is the application of an iterative procedure for elastic solutions, which allows for various manifestations of nonlinear deformation in the form of shear, stretching, friction along the surface of layers in a three-layer package, and the effect of delamination. As was previously accepted, the physical law of plastic deformations is the Mohr–Coulomb strength condition under compression with simultaneous shear, since the von Mises–Schleicher condition is more correctly applied in a spatial stressed state.

The main action in choosing the transition ratios of the subgrade soil from the elastic to the plastic state, required to determine the zones of the same deformation in the mixed problem of elasticity theory, is establishing the yield condition on the stress–strain plot constructed in the laboratory for this soil. The next step is the imitation of this plot in the finite element model (FE model) using an iterative procedure, during which the obtained solutions in the form of stresses $\{\sigma\}$ and strains $\{\varepsilon\}$ in tensor form are corrected in accordance with the "stress–strain" diagram. This procedure makes it possible to bring the deformation process in the FE model closer to the results of laboratory tests and thus achieve a sufficiently complete and detailed imitation of the properties of the subgrade soil. It should be emphasized that the filler material (crushed stone–soil mixture) was taken, as already mentioned above, to be elastic for the range of applied loads to simplify the calculations, which is proven by testing its physical and mechanical properties. The elastic formulation of the problem in subsequent analysis is justified by the test results of the ballast, subgrade, and the filling material, which demonstrate that within the range of train loads, only reversible (elastic) deformations occur.

Thus, zones with stresses not exceeding and exceeding the yield strength of the subgrade soil were determined during the iteration procedure. Accordingly, the iteration process for the elastic deformation zone was terminated, continuing for the plastic deformation zone. Moreover, at each step of the load increment in the iteration process, the possible growth of plastic deformation zones was monitored, since the potential redistribution of stresses can cause an increase in these areas.

Considering that the subgrade soil is accepted as a medium that practically does not resist stretching, an analysis of stresses that cause this type of deformation is carried out accordingly, accepting the assumption that cracks may appear perpendicular to the

formation of the main stress σ_1, and the second main stress must satisfy the condition $\sigma_2 \in \left(0; \frac{2Ccos\phi}{1-sin\phi}\right)$.

To compile the equations linking the stress tensors in the elastic $\{\sigma^e\}$ and plastic $\{\sigma^p\}$ deformation zones, the principle of elastic solutions was applied. According to this principle, the elastic deformations caused by the first tensor are equal to the elastic–plastic deformations caused by the second tensor. Then, for flat deformation conditions, the equations of connection take the following form:

$$\left.\begin{array}{l} \frac{1}{2G}\left[(1-\mu)\sigma_1^e - \mu\sigma_2^e\right] = \frac{1}{2G}\left[(1-\mu)\sigma_1^p - \mu\sigma_2^p\right] + \frac{\lambda}{2} \\ \frac{1}{2G}\left[(1-\mu)\sigma_2^e - \mu\sigma_1^e\right] = \frac{1}{2G}\left[(1-\mu)\sigma_2^p - \mu\sigma_1^p\right] + \frac{\lambda}{2} \end{array}\right\}, \quad (26)$$

where σ_1^e and σ_2^e are the principal stresses in the elastic deformation zone; σ_1^p and σ_2^p are the principal stresses in the plastic deformation zone; and λ is the small scalar exponent, according to Drucker–Prager.

The unknown principal stresses σ_1^p and σ_2^p must satisfy the yield condition:

$$F^p = \frac{\sigma_1^p - \sigma_2^p}{2} + \frac{\sigma_1^p + \sigma_2^p}{2} sin\phi - Ccos\phi = 0. \quad (27)$$

Equations (26) and (27) form a closed system, the solution to which allows us to obtain a small scalar exponent according to Drucker–Prager:

$$\left.\begin{array}{c} \lambda = \frac{F^e}{G} \\ \sigma_{1,2}^p = \sigma_{1,2}^e \mp F^e \end{array}\right\}, \quad (28)$$

where $F^e = \frac{\sigma_1^e - \sigma_2^e}{2} + \frac{\sigma_1^e + \sigma_2^e}{2} sin\phi - Ccos\phi$.

The determination of stress and strain tensors is performed after a full cycle of the iteration procedure with the defining elastic and plastic deformation areas and is a standard matrix operation of FEM, which is described in detail in many fundamental works and is not new. In practice, analytical provisions are further implemented in the professional licensed suite StructureCAD for Windows (SCAD), in which all numerical calculations for the reinforced subgrade are performed.

3. Results of Numerical Analysis of Combined Subgrade Reinforcement

3.1. Numerical Analysis of the Subgrade with Combined Reinforcement

The railway model was built using Structure CAD for Windows, version 7.29 R.3 (SCAD) (license number F755B84 (KMBKB RA 4810)). The model is represented by a fragment of the subgrade with a height of 6.0 m and the permanent way with a length of 0.2 m and consisting of elements of 0.05 × 0.05 × 0.05 m, Figure 6.

Table 1 gives the deformation characteristics of the model objects. The characteristics of the track superstructure are typical for reinforced concrete sleepers and UIC60 (or R65) rails, and with these values, they are used in many modern studies [6,29–32]. The characteristics of the ballast layer (crushed stone) can vary within a certain range depending on different factors [4,19,33,34]. For this study, the characteristics were assumed to approximate the minimum but acceptable strength values. The data for the subgrade were obtained by the authors during laboratory tests.

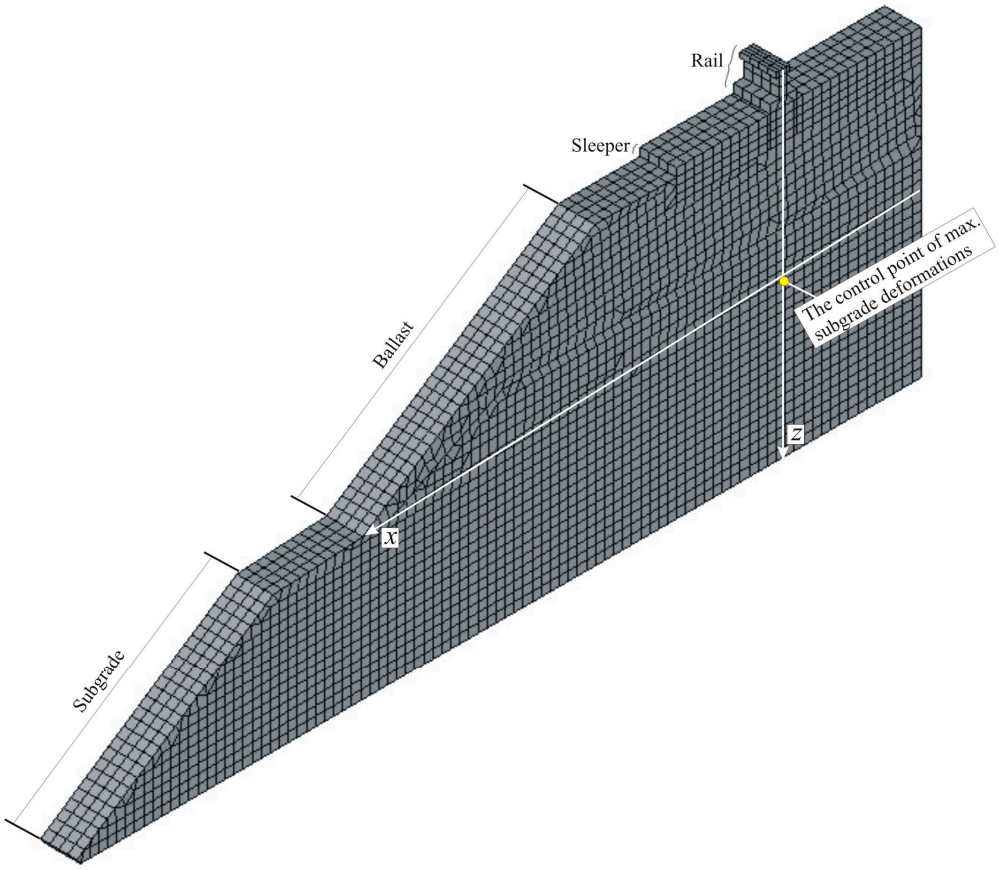

Figure 6. Fragment of a three-dimensional model.

Table 1. Deformation characteristics of the model's volumetric elements.

Model Element ID	Modulus of Elasticity, kPa	Poisson's Ratio	Volumetric Weight, kN/m^3
Rail	2.1×10^8	0.3	77.0
Sleeper	3.91×10^7	0.2	24.5
Crushed stone	10×10^4	0.2	20.0
Subgrade	35×10^3	0.3	20.0
Base	35×10^3	0.3	20.0
Crushed stone–soil mixture	12×10^4	0.2	22.5

The model is loaded with a vertical concentrated force of 98.1 kN applied to the rail. This corresponds to a static load from the wheel to the track at the level of 20 t/axle.

The calculation was carried out using the multi-frontal method, further refining the results considering the type of deformations (see Section 2.4).

Figure 7 shows the distribution of deformations on a fragment of the subgrade. The first version of calculations (Figure 7a) provides results for the subgrade without reinforcement; in the second option (Figure 7b), the subgrade is reinforced by the method of an open shell. The open shell (see Figure 1) is filled with a crushed stone–soil mixture and is located at a depth of 0.2 m from the main site.

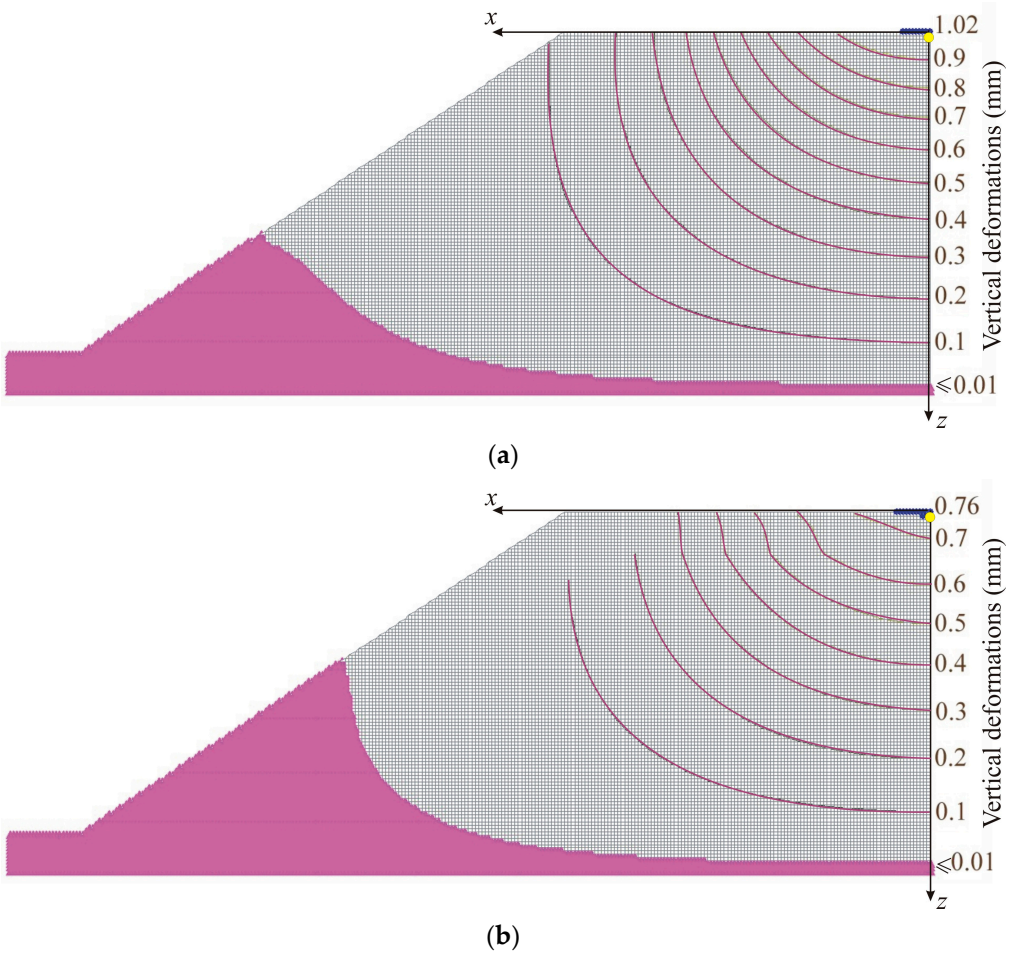

Figure 7. Vertical deformations (mm) of a fragment of the subgrade model under the action of a train load (**a**) without reinforcement and (**b**) with reinforcement (open shell).

The characteristics of the geotextile are as follows:

- Volumetric weight—11 kN/m^3;
- Modulus of elasticity—0.8 MPa;
- Poisson's ratio—0.35;
- Plate thickness—4 mm.

To represent the results of the deformed state, a special display filter embedded in the SCAD calculation package is applied. With its help, vertical deformations are displayed for all reinforcement options, and for each of them, a constant step of the deformation component between isolines is chosen (0.1 mm for vertical deformations). The main characteristic zones of vertical deformations shown in Figure 7 are a zone of value 0.01 m (represented by the magenta fill in the lower part) and a zone of maximum values (represented by the blue fill in the upper part). The first isoline of vertical deformations from the zone of zero values equals 0.1 mm. The nature of the distribution of isolines proves the perceptible influence of combined reinforcement, expressed in isoline fractures in the zone of an open geotextile shell with a compacted crushed stone–soil mixture. The results show that the maximum vertical deformations in the model without the geotextile are equal to 1.02 mm, and in the model with an open shell, the maximum is 0.76 mm.

Thus, from the results, it can be concluded that when using an open geotextile shell with a compacted crushed stone–soil mixture, the vertical displacements are reduced by 1.34 times, which characterizes the effectiveness of this option of reinforcing the subgrade.

3.2. Results of Analyzing the Parameters of Experimental Research on the Geotextile Reinforcement of the Subgrade

Experimental research was conducted in a flat tray designed at the Sectoral Research Laboratory of Soil Mechanics, the Ukrainian State University of Science and Technology, Figure 8a. The height of the tray was 220 mm, the dimensions in plan were 680 × 120 mm. In loading the models, the level of absolute deformations was monitored using time-type indicators, Figure 8b.

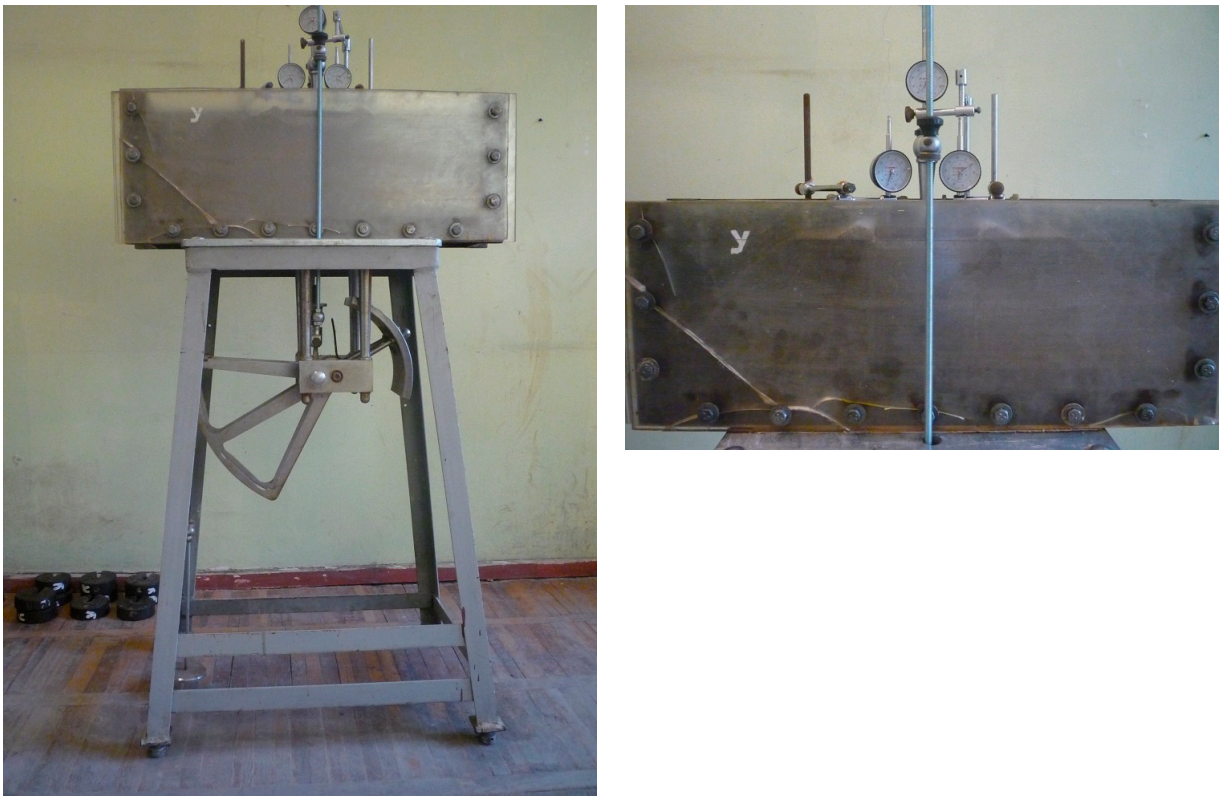

(**a**) (**b**)

Figure 8. The set-up for experimenting: (**a**) general view of a flat tray; (**b**) the structure of the working area with a model and measuring devices.

The primary challenge that may arise during the implementation of the combined reinforcement method is the effect of the scale factor. This factor slightly adjusts the data obtained during physical modeling on a small-scale model. To thoroughly assess the impact of the scale factor, it is necessary to conduct tests on an experimental section of the subgrade with combined reinforcement and compare the results with laboratory experiment data.

A metal ball with a diameter of 8 mm was installed in the model's center to ensure vertical load transfer. The vertical load on the stamp was created using laboratory weights (4 kg), while the load was transmitted using a lever system with a 1:10 arm through a rigid metal stamp with an area of 0.016 m^2 (160.0 cm^2). The vertical load on the stamp increased from 40 to 80 N (considering the arm of the lever, from 400 to 800 N, respectively), while the stress under the stamp varied from 0.025 MPa to 0.05 MPa.

The vertical deformations of the stamp, which modeled the rail-sleeper grid, were recorded after adding each load level by photographing the deformed model and removing it according to the indicators of the readings, after which the average value was found.

The movement of the subgrade model was recorded by the graph paper rulers pasted on the side faces of the flat tray, as well as by the deformations of the model with a grid applied on its front side. To observe the evolution of deformations, a grid of 2.0 × 2.0 cm

was applied on the side of the transparent wall, drawn on the front side of the model with a sharp pencil on the leveled surface.

Dry soil (loam) was used to make the clay paste used for the tray experiments. The soil was soaked with water and passed through a set of sieves with a diameter of residues from 1.0 mm to 0.3 mm. The soil was placed in the tray in layers about 3.0 cm thick and compacted by tamping. When the thickness of the total layer in the tray reached 20 cm, the upper face of the model was leveled.

The mechanical properties of the soil were determined under laboratory conditions. For compression tests, its samples were taken from the tray. Compression tests are appropriate in this case for simulating the deformation of the subgrade, as the soil and soil–crushed stone mixture deform primarily under lateral compression within the embankment body. Furthermore, the influence of the testing apparatus conditions is minimal in compression tests because the sample's integrity is preserved. The physical and mechanical characteristics of the base soil are as follows: loam with a fluidity index of 0.05; plasticity number 0.135; soil density during model manufacturing 1.88–1.91 g/cm^3; density of dry soil l.269–l.287 g/cm^3; humidity 0.15–0.19; porosity coefficient 0.642–0.909; degree of humidity 0.65; and the modulus of deformation 34.8 MPa, which is almost identical to the modulus of deformation adopted for the numerical analysis by the finite element method described above.

A characteristic deformation of the subgrade model without reinforcement is the case of the creation of a compression core under the stamp, which is observed by the curvature of the grid, Figure 9.

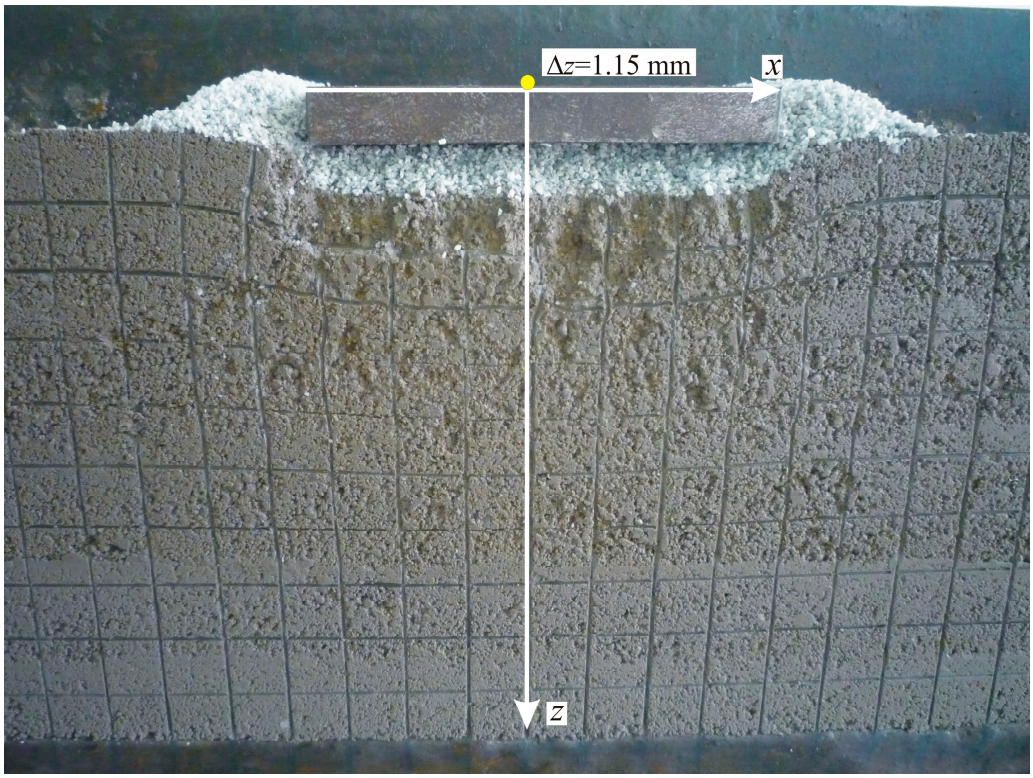

Figure 9. General view of the subgrade without reinforcement after the end of the experiment.

The deformation of models with reinforcement in the form of an open shell can be characterized as homogeneous, since no critical deformations in the form of delamination and pulling out of the reinforcement were detected. Strengthening following this option is rational, since a zone of over-compacted soil is formed inside the open shell, which absorbs most of the deformations of the compression core, and the bends do not allow the reinforcement to pull out, Figure 10.

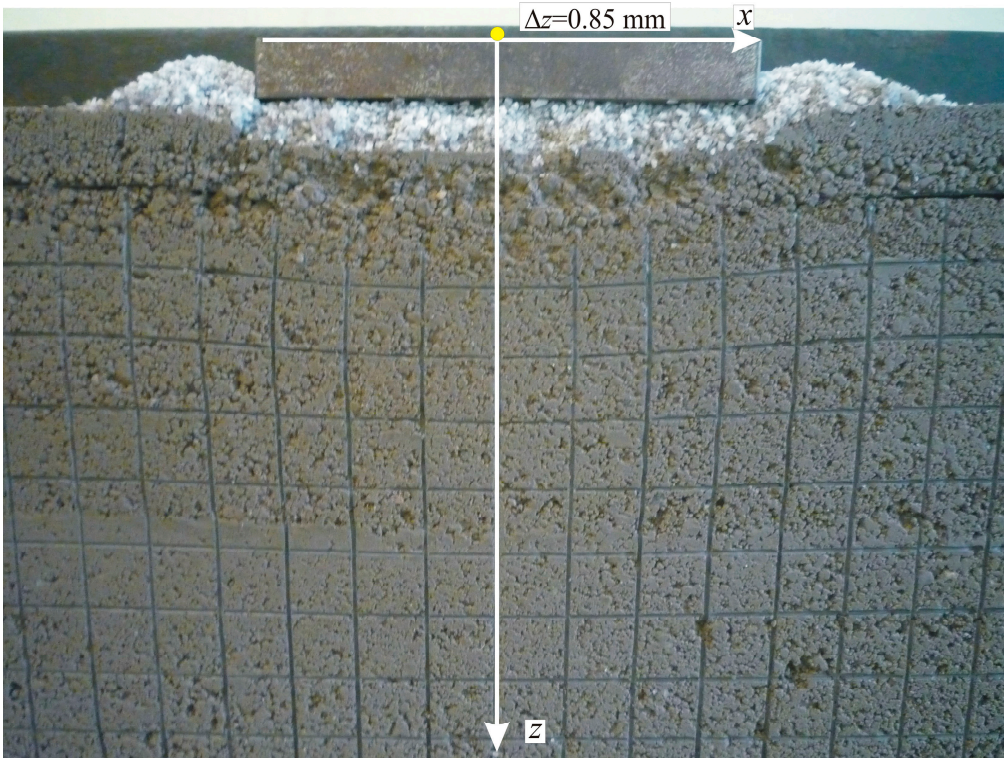

Figure 10. General view of the subgrade with reinforcement in the form of an open shell after the end of the experiment.

The nature of the deformation of models without reinforcement (see Figure 9) and with reinforcement in the form of an open shell differs in that the vertical lines of the 2.0 × 2.0 cm grid in the case of the reinforced model undergo less bending. This is explained by the fact that the open shell redistributes deformations due to its design. Such a shell is equally loaded and uniformly deformable.

However, the deformation of such a system during the tray experiment made it possible to determine some effects that were not considered in theoretical studies, Figure 11.

At the ends of the closed shell, due to the flexibility of its upper part being very limited by the formed overlap, insignificant delamination appeared. Such an effect, determined as a result of experimental studies, can be reduced by deepening the open shell into the body of the subgrade.

The results of experimental studies in the tray show that the maximum vertical deformations in the model without geotextiles are equal to 1.15 mm, and in the model with an open shell, they are 0.85 mm. From experimental studies, it can be concluded that when using an open geotextile shell with a compacted crushed stone–soil mixture, vertical deformations are reduced by 1.35 times. Comparing these results with the corresponding data from the numerical analysis shows a difference of 11.8–12.7%. This testifies to the correspondence of the numerical analysis and experimental studies in the tray, as well as the effectiveness of reducing the deformed state of the subgrade when using combined reinforcement.

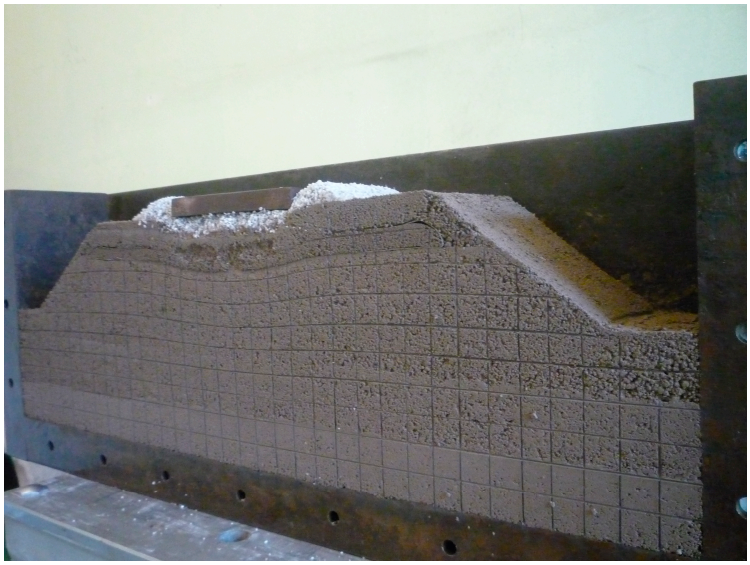

Figure 11. Peculiarities of deformation of the subgrade with reinforcement in the form of an open shell after the end of the experiment.

4. Discussion

The results of comprehensive research on the combined reinforcement of railway subgrades indicate that the use of geosynthetic materials has the potential as a means of strengthening. It was proved that the proposed structure, in the form of an open shell of geosynthetic material, inside which there is a layer of compacted crushed stone, effectively reduces the level of vertical deformations of the subgrade.

This method has a wide range of practical applications. Among other things, the authors consider the possibility of its use for soil reinforcement during significant structural changes in railway tracks, such as the transition from national to European track gauges (specifically to a combined structure with a dual gauge) [35], as an alternative to the use of micropiles and other means [21].

Provisions of the analytical method devised for combined reinforcement demonstrate that the direction of combining geosynthetic materials and a layer of compacted crushed stone is fruitful and requires further development. Research into this area can be divided into two tasks, namely (1) a parametric analysis of combined reinforcement, that is, finding out its effective parameters (thickness, modulus of elasticity of the compacted layer, changing the material of this layer, placement of combined reinforcement along the height of the subgrade, etc.) and (2) the theoretical substantiation of the uniformity of stresses and deformations of the combined reinforcement with the search for zones of bending the geosynthetic material and frictional forces on its surface. To enhance and provide greater detail in numerical modeling, future research can account for track irregularities and the dynamic impact of the train.

In further research, based on the results reported in this manuscript, it is possible to revise the theory of applying geosynthetic materials from the standpoint of their effectiveness depending on the structure (horizontal location, location with bending, anchored location, etc.). Such a revision could make it possible to reveal the existing potential of geosynthetic materials in the field of strengthening the subgrade of railways.

Modification of the proposed combined subgrade reinforcement system is possible by replacing the geosynthetic material of the unsealed shell from the fabric to the geogrid. Such a modification, due to the higher strength and stiffness of the geogrid, will enhance the overall strength and stiffness of the combined reinforcement. This improvement in key operational parameters will help account for the effects of extreme weather conditions or seasonal changes.

5. Conclusions

The concepts of subgrade reinforcement have been analyzed; the results prove that using geosynthetic materials has the appropriate potential. The advantages and disadvantages of the subgrade reinforcement concepts have been defined.

The paper devises the basics of the analytical method for determining the stress–strain state of the railway subgrade, which is reinforced with geosynthetic material. The reinforcement in this paper is combined, since the geosynthetic material is folded into an open shell, inside which there is a layer of compacted crushed stone.

Dependences of the general stress–strain state of the combined reinforcement in the form of an open shell of geosynthetic material, inside which there is a layer of compacted crushed stone, were implemented in numerical analysis, the results of which confirm the positive impact on the reduction in subgrade deformation.

The results of numerical analysis and experimental research prove that when using an open geotextile shell with a compacted crushed stone–soil mixture, vertical deformations are reduced by 1.34–1.35 times, which characterizes the effectiveness of this option for strengthening the subgrade.

Author Contributions: Conceptualization, A.A. and O.T.; methodology, O.T., S.F. and D.K.; software, O.T.; validation, D.K.; formal analysis, O.T. and S.F.; resources, A.A. and O.T.; writing—original draft preparation, O.T., S.F. and D.K.; writing—review and editing, A.A., S.F. and D.K.; visualization, O.T.; supervision, A.A. and S.F.; project administration, O.T. and S.F. All authors have read and agreed to the published version of the manuscript.

Funding: This research received no external funding.

Data Availability Statement: Data are contained within the article.

Acknowledgments: This research was facilitated by The National Research Foundation of Ukraine under the project "Scientific Justification of the Introduction of the European Track on the Territory of Ukraine in the Post-War Period" (project registration number 2022.01/0021), which was obtained through the "Science for the Recovery of Ukraine in the War and Post-War Periods" competition. The authors express gratitude to the employees of the Ukrainian State University of Science and Technologies and the members of the "SZE-RAIL" research team and the Vehicle Industry Research Center at Széchenyi István University.

Conflicts of Interest: The authors declare no conflicts of interest.

References

1. Xu, F.; Yang, Q.; Liu, W.; Leng, W.; Nie, R.; Mei, H. Dynamic Stress of Subgrade Bed Layers Subjected to Train Vehicles with Large Axle Loads. *Shock Vib.* **2018**, *2018*, 2916096. [CrossRef]
2. Chumyen, P.; Connolly, D.P.; Woodward, P.K.; Markine, V. A comparison of earthwork designs for railway transition zones. *Constr. Build. Mater.* **2023**, *395*, 132295. [CrossRef]
3. Nålsund, R. Effect of Grading on Degradation of Crushed-Rock Railway Ballast and on Permanent Axial Deformation. *Transp. Res. Rec.* **2010**, *2154*, 149–155. [CrossRef]
4. Sysyn, M.; Kovalchuk, V.; Gerber, U.; Nabochenko, O.; Pentsak, A. Experimental study of railway ballast consolidation inhomogeneity under vibration loading. *Pollack Period.* **2020**, *15*, 27–36. [CrossRef]
5. Ézsiás, L.; Tompa, R.; Fischer, S. Investigation of the Possible Correlations Between Specific Characteristics of Crushed Stone Aggregates. *Spectr. Mech. Eng. Oper. Res.* **2024**, *1*, 10–26. [CrossRef]
6. Kurhan, D.; Kurhan, M.; Horváth, B.; Fischer, S. Determining the Deformation Characteristics of Railway Ballast by Mathematical Modeling of Elastic Wave Propagation. *Appl. Mech.* **2023**, *4*, 803–815. [CrossRef]
7. Sysyn, M.; Przybylowicz, M.; Nabochenko, O.; Liu, J. Mechanism of Sleeper–Ballast Dynamic Impact and Residual Settlements Accumulation in Zones with Unsupported Sleepers. *Sustainability* **2021**, *13*, 7740. [CrossRef]
8. Chalabii, J.; Esmaeili, M.; Gosztola, D.; Fischer, S.; Movahedi Rad, M. Effect of the Particle Size Distribution of the Ballast on the Lateral Resistance of Continuously Welded Rail Tracks. *Infrastructures* **2024**, *9*, 129. [CrossRef]
9. Hoque, I.L.; Aziz, S.; Mallick, J.R.; Nayeem, M.A.; Maisha, T.E.H.; Hossain, F.M.Z.; Amin, A.F.M.S. Response Analysis of a Ballasted Rail Track Constructed on Soft Soil by 3D Modeling. *Adv. Civ. Eng.* **2023**, *1*, 4290824. [CrossRef]
10. Nabochenko, O.; Sysyn, M.; Gerber, U.; Krumnow, N. Analysis of Track Bending Stiffness and Loading Distribution Effect in Rail Support by Application of Bending Reinforcement Methods. *Urban Rail Transit* **2023**, *9*, 73–91. [CrossRef]

11. Elliott, R.P.; Dennis, N.D.; Qiu, Y. *Permanent Deformation of Subgrade Soils*; Mack-Blackwell Transportation Center: Fayetteville, NC, USA, 1998; 216p.
12. Ižvolt, L.; Dobeš, P.; Pultznerová, A. Monitoring of moisture changes in the construction layers of the railway substructure body and its subgrade. *Procedia Eng.* **2016**, *161*, 1049–1056. [CrossRef]
13. Alabbasi, Y.; Hussein, M. Geomechanical Modelling of Railroad Ballast: A Review. *Arch. Comput. Methods Eng.* **2021**, *28*, 815–839. [CrossRef]
14. Volkov, V.; Taran, I.; Volkova, T.; Pavlenko, O.; Berezhnaja, N. Determining the Efficient Management System for a Specialized Transport Enterprise. *Nauk. Visnyk Natsionalnoho Hirnychoho Universytetu* **2020**, *2020*, 185–191. [CrossRef]
15. Saukenova, I.; Oliskevych, M.; Taran, I.; Toktamyssova, A.; Aliakbarkyzy, D.; Pelo, R. Optimization of Schedules for Early Garbage Collection and Disposal in the Megapolis. *East.-Eur. J. Enterp. Technol.* **2022**, *1*, 13–23. [CrossRef]
16. Fischer, S.; Kocsis Szürke, S. Detection Process of Energy Loss in Electric Railway Vehicles. Facta Universitatis. *Ser. Mech. Eng.* **2023**, *21*, 81–99. [CrossRef]
17. Kuchak, A.T.J.; Marinkovic, D.; Zehn, M. Finite Element Model Updating—Case Study of a Rail Damper. *Struct. Eng. Mech.* **2020**, *73*, 27–35. [CrossRef]
18. Desbrousses, R.L.E.; Meguid, M.A.; Bhat, S. Experimental Investigation of the Effects of Subgrade Strength and Geogrid Location on the Cyclic Response of Geogrid-Reinforced Ballast. *Int. J. Geosynth. Ground Eng.* **2023**, *9*, 67. [CrossRef]
19. Fischer, S. Geogrid reinforcement of ballasted railway superstructure for stabilization of the railway track geometry—A case study. *Geotext. Geomembr.* **2022**, *50*, 1036–1051. [CrossRef]
20. Hussaini, S.K.K.; Sweta, K. Investigation of deformation and degradation response of geogrid-reinforced ballast based on model track tests. *Proc. Inst. Mech. Eng. Part F J. Rail Rapid Transit* **2021**, *235*, 505–517. [CrossRef]
21. Tiutkin, O.; Autelitano, F.; Giuliani, F.; Neduzha, L. Stress-strain behavior of railway embankments stabilized with grouted micropiles. *Alex. Eng. J.* **2024**, *102*, 75–81. [CrossRef]
22. Tiutkin, O.L.; Neduzha, L.; Kalivoda, J. Finite-element Analysis of Strengthening the Subgrade on the Basis of Boring and Mixing Technology. *Transp. Probl.* **2021**, *16*, 189–197. [CrossRef]
23. Senkaya, A.; Toka, E.B.; Olgun, M. Effects of Cement Grout Characteristics on Formation and Strength of Jet Grouting Columns. *Arab. J. Sci. Eng.* **2022**, *47*, 13035–13047. [CrossRef]
24. Iwański, M.; Chomicz-Kowalska, A. Application of the foamed bitumen and bitumen emulsion to the road base mixes in the deep cold recycling technology. *Balt. J. Road Bridge Eng.* **2016**, *11*, 291–301. [CrossRef]
25. Xin, X.; Degou, C.; Liangwei, L.; Yuefeng, S.; Feipeng, X. Application of asphalt based materials in railway systems: A review. *Constr. Build. Mater.* **2021**, *304*, 124630. [CrossRef]
26. Fiore, N.; Bruno, S.; Del Serrone, G.; Iacobini, F.; Giorgi, G.; Rinaldi, A.; Moretti, L.; Duranti, G.M.; Peluso, P.; Vita, L.; et al. Experimental Analysis of Hot-Mix Asphalt (HMA) Mixtures with Reclaimed Asphalt Pavement (RAP) in Railway Sub-Ballast. *Materials* **2023**, *16*, 1335. [CrossRef]
27. Alsirawan, R.; Koch, E. Dynamic Analysis of Geosynthetic-reinforced Pile-supported Embankment for a High-Speed Rail. *Acta Polytech. Hung.* **2024**, *21*, 31–50. [CrossRef]
28. Liu, C.; Shan, Y.; Wang, B.; Zhou, S.; Wang, C. Reinforcement load in geosynthetic-reinforced pile-supported model embankments. *Geotext. Geomembr.* **2022**, *50*, 1135–1146. [CrossRef]
29. Auersch, L. Reduction of Train-Induced Vibrations—Calculations of Different Railway Lines and Mitigation Measures in the Transmission Path. *Appl. Sci.* **2023**, *13*, 6706. [CrossRef]
30. de Melo, A.L.O.; Kaewunruen, S.; Li, T.; Goto, K. Non-linear influences of track dynamic irregularities on vertical levelling loss of heavy-haul railway track geometry under cyclic loadings. *Nonlinear Eng.* **2024**, *13*, 20240011. [CrossRef]
31. Muradian, L.; Shvets, A.; Shvets, A. Influence of wagon body flexural deformation on the indicators of interaction with the railroad track. *Arch. Appl. Mech.* **2024**, *94*, 2201–2216. [CrossRef]
32. Kuchak, A.J.T.; Marinkovic, D.; Zehn, M. Parametric Investigation of a Rail Damper Design Based on a Lab-Scaled Model. *J. Vib. Eng. Technol.* **2021**, *9*, 51–60. [CrossRef]
33. Hua, X.; Zatar, W.; Cheng, X.; Chen, G.S.; She, Y.; Xu, X.; Liao, Z. Modeling and Characterization of Complex Dynamical Properties of Railway Ballast. *Appl. Sci.* **2024**, *14*, 11224. [CrossRef]
34. Liu, J.; Liu, Z.; Wang, P.; Kou, L.; Sysyn, M. Dynamic characteristics of the railway ballast bed under water-rich and low-temperature environments. *Eng. Struct.* **2022**, *252*, 113605. [CrossRef]
35. Fischer, S.; Kurhan, D.; Kurhan, M.; Hmelevska, N. Analysis of stress-strain state changes in railway tracks during transition to European gauge. *IOP Conf. Ser. Earth Environ. Sci.* **2024**, *1348*, 012029. [CrossRef]